ATTACHMENT 4

CDI REPORT 08-08NP (NON-PROPRIETARY), ACOUSTIC AND LOW FREQUENCY HYDRODYNAMIC LOADS AT CLTP POWER LEVEL ON NINE MILE POINT UNIT 2 STEAM DRYER TO 250 HZ, REV. 3 (LAR ATTACHMENT 13.8)

Certain information, considered proprietary by CDI, has been deleted from this Attachment. The deletions are identified by double square brackets.

This Document Does Not Contain Continuum Dynamics, Inc. Proprietary Information

C.D.I. Report No. 08-08NP

Acoustic and Low Frequency Hydrodynamic Loads at CLTP Power Level on Nine Mile Point Unit 2 Steam Dryer to 250 Hz

Revision 3

Prepared by

Continuum Dynamics, Inc.
34 Lexington Avenue
Ewing, NJ 08618

Prepared under Purchase Order No. 7708631 for

Constellation Energy Group
Nine Mile Point Nuclear Station, LLC
P. O. Box 63
Lycoming, NY 13093

Approved by

Alan J. Bilanin

Prepared by

Milton E. Teske

December 2009

This Document Does Not Contain Continuum Dynamics, Inc. Proprietary Information

Executive Summary

Measured strain gage time-history data in the four main steam lines at Nine Mile Point Unit 2 were processed by a dynamic model of the steam delivery system to predict loads on the full-scale steam dryer. These measured data were first converted to pressures, then positioned on the four main steam lines and used to extract acoustic sources in the system. A validated acoustic circuit methodology was used to predict the fluctuating pressures anticipated across components of the steam dryer in the reactor vessel. The acoustic circuit methodology included a low frequency hydrodynamic contribution, in addition to an acoustic contribution at all frequencies. This pressure loading was then provided for structural analysis to assess the structural adequacy of the steam dryer in Nine Mile Point Unit 2.

This effort provides the Constellation Energy Group with a dryer dynamic load definition that comes directly from measured Nine Mile Point Unit 2 full-scale data and the application of a validated acoustic circuit methodology, at a power level where data were acquired.

Table of Contents

Section		Page
	Executive Summary	i
	Table of Contents	ii
1.	Introduction	1
2.	Modeling Considerations	2
	2.1 Helmholtz Analysis	2
	2.2 Acoustic Circuit Analysis	3
	2.3 Low Frequency Contribution	4
3.	Input Pressure Data	5
4.	Results	15
5.	Uncertainty Analysis	23
6.	Conclusions	25
7.	References	26

1. Introduction

In Spring 2005 Exelon installed new stream dryers into Quad Cities Unit 2 (QC2) and Quad Cities Unit 1. This replacement design, developed by General Electric, sought to improve dryer performance and overcome structural inadequacies identified on the original dryers, which had been in place for the last 30 years. As a means for confirming the adequacy of the steam dryer, the QC2 replacement dryer was instrumented with pressure sensors at 27 locations. These pressures formed the set of data used to validate the predictions of an acoustic circuit methodology under development by Continuum Dynamics, Inc. (C.D.I.) for several years [1]. One of the results of this benchmark exercise [2] confirmed the predictive ability of the acoustic circuit methodology for pressure loading across the dryer, with the inclusion of a low frequency hydrodynamic load. This methodology, validated against the Exelon full-scale data and identified as the Modified Bounding Pressure model, is used in the effort discussed herein.

This report applies this validated methodology to the Nine Mile Point Unit 2 (NMP2) steam dryer and main steam line geometry. Strain gage data obtained from the four main steam lines were used to predict pressure levels on the NMP2 full-scale dryer at Current Licensed Thermal Power (CLTP). These data were then used to predict dryer stresses, and to determine the minimum stress margin on the dryer. This result will then be used to develop limit curves, a sample of which is shown in the Appendix.

2. Modeling Considerations

The acoustic circuit analysis of the NMP2 steam supply system is broken into two distinct analyses: a Helmholtz solution within the steam dome and an acoustic circuit analysis in the main steam lines. This section of the report highlights the two approaches taken here. These analyses are then coupled for an integrated solution.

2.1 Helmholtz Analysis

A cross-section of the steam dome (and steam dryer) is shown below in Figure 2.1, with NMP2 dimensions as shown [3]. The complex three-dimensional geometry is rendered onto a uniformly-spaced rectangular grid (with mesh spacing of approximately 1.5 inches to accommodate frequency from 0 to 250 Hz in full scale), and a solution, over the frequency range of interest, is obtained for the Helmholtz equation

$$\frac{\partial^2 P}{\partial x^2}+\frac{\partial^2 P}{\partial y^2}+\frac{\partial^2 P}{\partial z^2}+\frac{\omega^2}{a^2}P=\nabla^2 P+\frac{\omega^2}{a^2}P=0$$

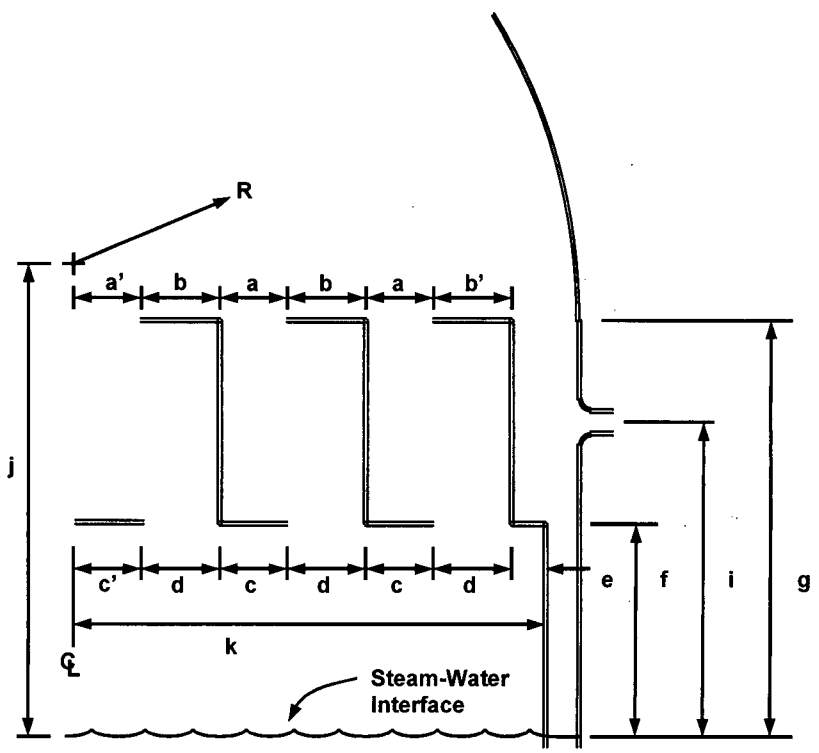

Figure 2.1. Cross-sectional description of the steam dome and dryer at NMP2, with the dimensions of a = 18.25 in, a' = 15.25 in, b = 13.27 in, b' = 13.65 in, c = 15.75 in, c' = 24.0 in, d = 15.75 in, e = 16.25 in, f = 71.5 in, g = 160.625 in, i = 84.5 in, j = 181.5 in, k = 118.75 in, and R = 124.75 in.

where P is the pressure at a grid point, ω is frequency, and a is acoustic speed in steam.

This equation is solved for incremental frequencies from 0 to 250 Hz (full scale), subject to the boundary conditions

$$\frac{dP}{dn} = 0$$

normal to all solid surfaces (the steam dome wall and interior and exterior surfaces of the dryer),

$$\frac{dP}{dn} \propto \frac{i\omega}{a} P$$

normal to the nominal water level surface, and unit pressure applied to one inlet to a main steam line and zero applied to the other three.

2.2 Acoustic Circuit Analysis

The Helmholtz solution within the steam dome is coupled to an acoustic circuit solution in the main steam lines. Pulsation in a single-phase compressible medium, where acoustic wavelengths are long compared to transverse dimensions (directions perpendicular to the primary flow directions), lend themselves to application of the acoustic circuit methodology. If the analysis is restricted to frequencies below 250 Hz, acoustic wavelengths are approximately 8 feet in length and wavelengths are therefore long compared to most components of interest, such as branch junctions.

Acoustic circuit analysis divides the main steam lines into elements which are each characterized, as sketched in Figure 2.2, by a length L, a cross-sectional area A, a fluid mean density $\bar{\rho}$, a fluid mean flow velocity $\bar{U}$, and a fluid mean acoustic speed $\bar{a}$.

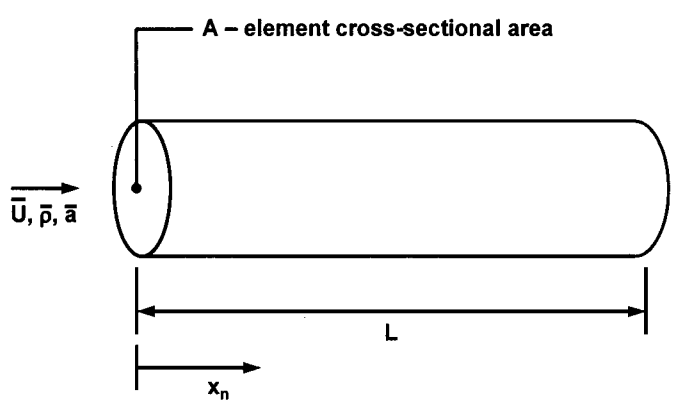

Figure 2.2. Schematic of an element in the acoustic circuit analysis, with length L and cross-sectional area A.

Application of acoustic circuit methodology generates solutions for the fluctuating pressure P_n and velocity u_n in the nth element of the form

$$P_n = \left[A_n e^{ik_{1n}X_n} + B_n e^{ik_{2n}X_n}\right] e^{i\omega t}$$

$$u_n = -\frac{1}{\rho \bar{a}^2}\left[\frac{\left(\omega + \bar{U}_n k_{1n}\right)}{k_{1n}} A_n e^{ik_{1n}X_n} + \frac{\left(\omega + \bar{U}_n k_{2n}\right)}{k_{2n}} B_n e^{ik_{2n}X_n}\right] e^{i\omega t}$$

where harmonic time dependence of the form $e^{i\omega t}$ has been assumed. The wave numbers k_{1n} and k_{2n} are the two complex roots of the equation

$$k_n^{\,2} + i\frac{f_n\left|\bar{U}_n\right|}{D_n \bar{a}^2}\left(\omega + \bar{U}_n k_n\right) - \frac{1}{\bar{a}^2}\left(\omega + \bar{U}_n k_n\right)^2 = 0$$

where f_n is the pipe friction factor for element n, D_n is the hydrodynamic diameter for element n, and $i = \sqrt{-1}$. A_n and B_n are complex constants which are a function of frequency and are determined by satisfying continuity of pressure and mass conservation at element junctions.

The solution for pressure and velocity in the main steam lines is coupled to the Helmholtz solution in the steam dome, to predict the pressure loading on the steam dryer.

The main steam line piping geometry is summarized in Table 2.1.

Table 2.1. Main steam line lengths at NMP2, measured from the inside wall of the steam dome down the centerline of the main steam lines. Main steam line diameter is 26 inch Schedule 80 (ID = 23.50 in).

Main Steam Line	Length to First Strain Gage Measurement (ft)	Length to Second Strain Gage Measurement (ft)
A	13.6	26.2
B	14.5	19.9
C	22.1	27.5
D	20.4	25.8

2.3 Low Frequency Contribution

[[

(3)]]

3. Input Pressure Data

Strain gages were mounted on the four main steam lines of NMP2. Two data sets were examined in this analysis. The first data set recorded the strain at Current Licensed Thermal Power (100% power level or CLTP), and the second data set recorded the strain at near-zero voltage on the strain gages (EIC noise at CLTP). The data were provided in the following files:

Data File Name	Power Level	Voltage
20080419094734	100%	10.0 V
20080419094134	100%	0.01 V (EIC)

The strain gage signals were converted to pressures by the use of the conversion factors provided in [4] and summarized in Table 3.1. Exclusion frequencies were used to remove extraneous signals, as also identified in [4] and [5], and summarized in Table 3.2. The electrical noise was removed by applying the function

$$P_S(\omega) = P_{SN}(\omega)\left[1 - \left|\frac{P_N(\omega)}{P_{SN}(\omega)}\right|\right]$$

where $P_S(\omega)$ is the CLTP signal $P_{SN}(\omega)$ corrected for electrical noise $P_N(\omega)$, computed as a function of frequency ω, and $|P_N(\omega)/P_{SN}(\omega)|$ can be no larger than 1.0. The strain gage signals, converted to pressures, are shown in Figure 3.1, comparing CLTP (P_{SN}), EIC (P_N), and CLTP – EIC (P_S) signals before exclusion frequency filtering.

CLTP signals were further processed by the coherence factor and mean filtering as described in [2]. Coherence is shown in Figure 3.2.

The resulting main steam line pressure signals may be represented in two ways, by their minimum and maximum pressure levels, and by their PSDs. Table 3.3 provides the pressure level information, while Figure 3.3 compares the CLTP frequency content at the eight measurement locations.

Table 3.1. Conversion factors from strain to pressure [4]. Channels are averaged to give the average strain; blank sensors indicate that the sensor was inoperative.

	Strain to Pressure (psid/μstrain)	Channel Number	Channel Number	Channel Number	Channel Number
MSL A Upper	3.82	1	2	3	
MSL A Lower	3.84	5	6	7	8
MSL B Upper	3.84	9	10	11	12
MSL B Lower	3.81	13	14	15	16
MSL C Upper	3.85	17	18	19	20
MSL C Lower	3.81	21	22	23	24
MSL D Upper	3.92	15	26	27	
MSL D Lower	3.94	29	30	31	32

Table 3.2. Exclusion frequencies for NMP2 strain gage data, as suggested in [4] and [5].

Frequency Range (Hz)	Exclusion Cause
0.0 – 2.0	Mean
58.85 – 60.15	Line Noise
119.9 – 120.1	Line Noise
179.6 – 180.4	Line Noise
239.8 – 240.2	Line Noise
148.85 – 149.15	Recirculation Vane Passing Frequency: 100%
87.9 – 88.1	Extraneous Non Identified Electrical Source
112.8 – 113.2	Extraneous Non Identified Electrical Source
134.1 – 134.9	Extraneous Non Identified Electrical Source
27.9 – 28.1; 33.5 – 34.5	MSL A Pipe Vibrations
68.9 – 71.1; 79.9 – 81.1	MSL B Pipe Vibrations
12.7 – 13.4	MSL C Pipe Vibrations
39.6 – 40.4; 91.2 – 91.6	MSL D Pipe Vibrations

Table 3.3. Main steam line (MSL) pressure levels in NMP2 at CLTP conditions.

	Minimum Pressure (psid)	Maximum Pressure (psid)	RMS Pressure (psid)
MSL A Upper	-1.55	1.59	0.35
MSL A Lower	-1.88	2.07	0.46
MSL B Upper	-1.63	1.47	0.37
MSL B Lower	-1.54	1.34	0.32
MSL C Upper	-2.09	1.99	0.51
MSL C Lower	-1.74	1.76	0.43
MSL D Upper	-1.86	1.72	0.40
MSL D Lower	-1.76	1.63	0.40

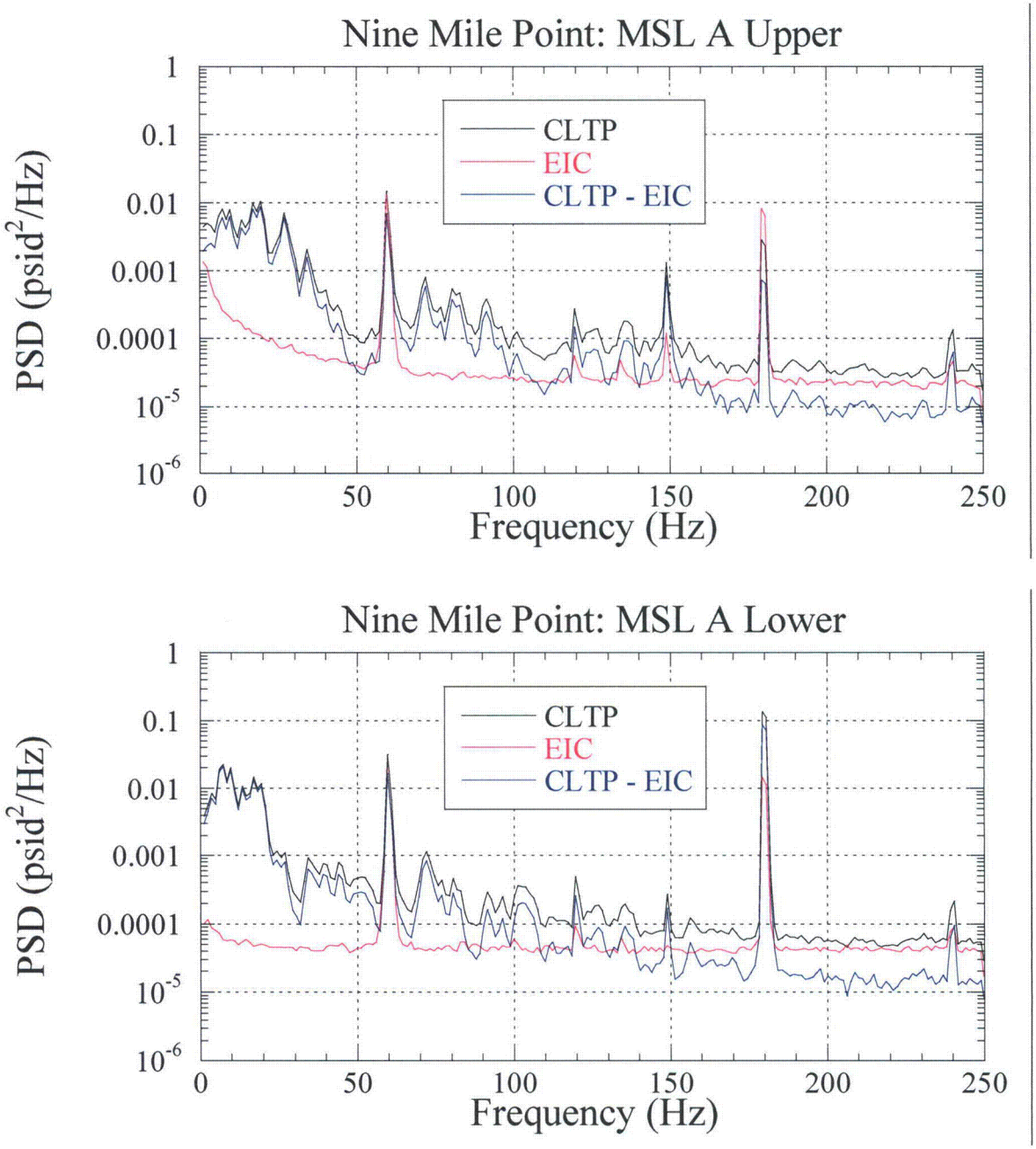

Figure 3.1a: Comparison of unfiltered data measured on the NMP2 main steam lines at CLTP conditions (black curves), EIC (red curves), and subtraction of EIC from CLTP (blue curves: MSL A Upper (top); MSL A Lower (bottom).

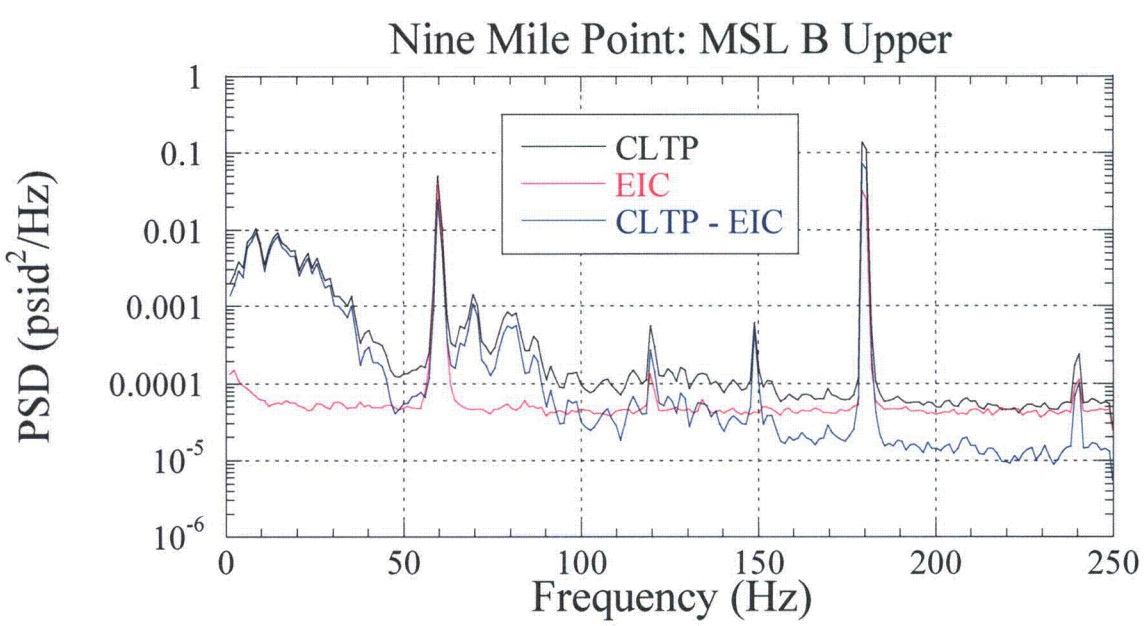

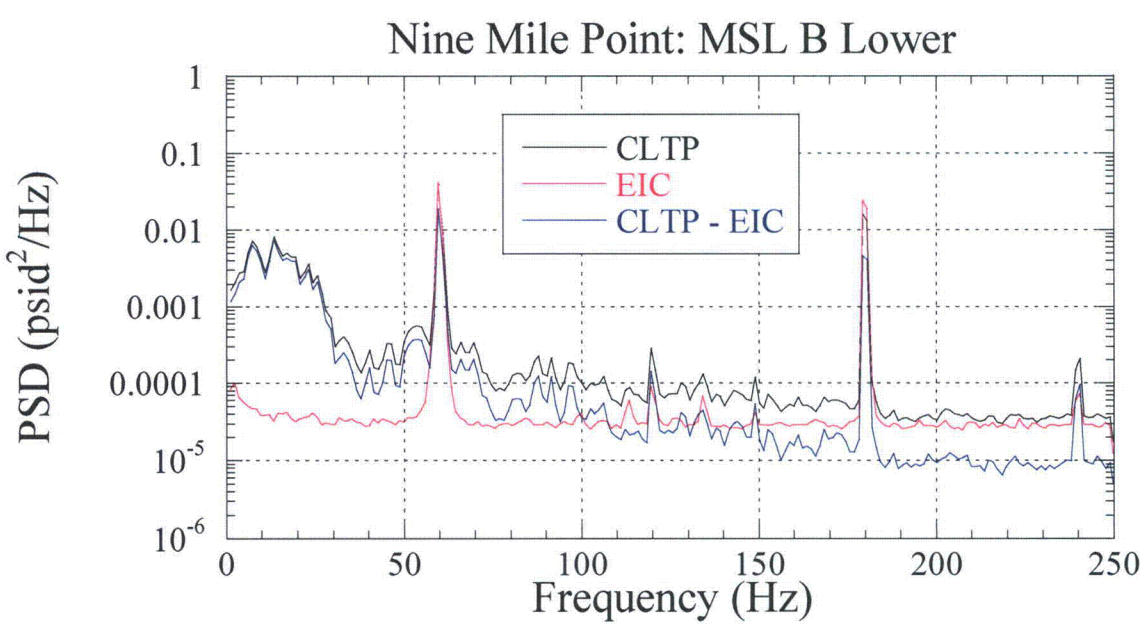

Figure 3.1b: Comparison of unfiltered data measured on the NMP2 main steam lines at CLTP conditions (black curves), EIC (red curves), and subtraction of EIC from CLTP (blue curves: MSL B Upper (top); MSL B Lower (bottom).

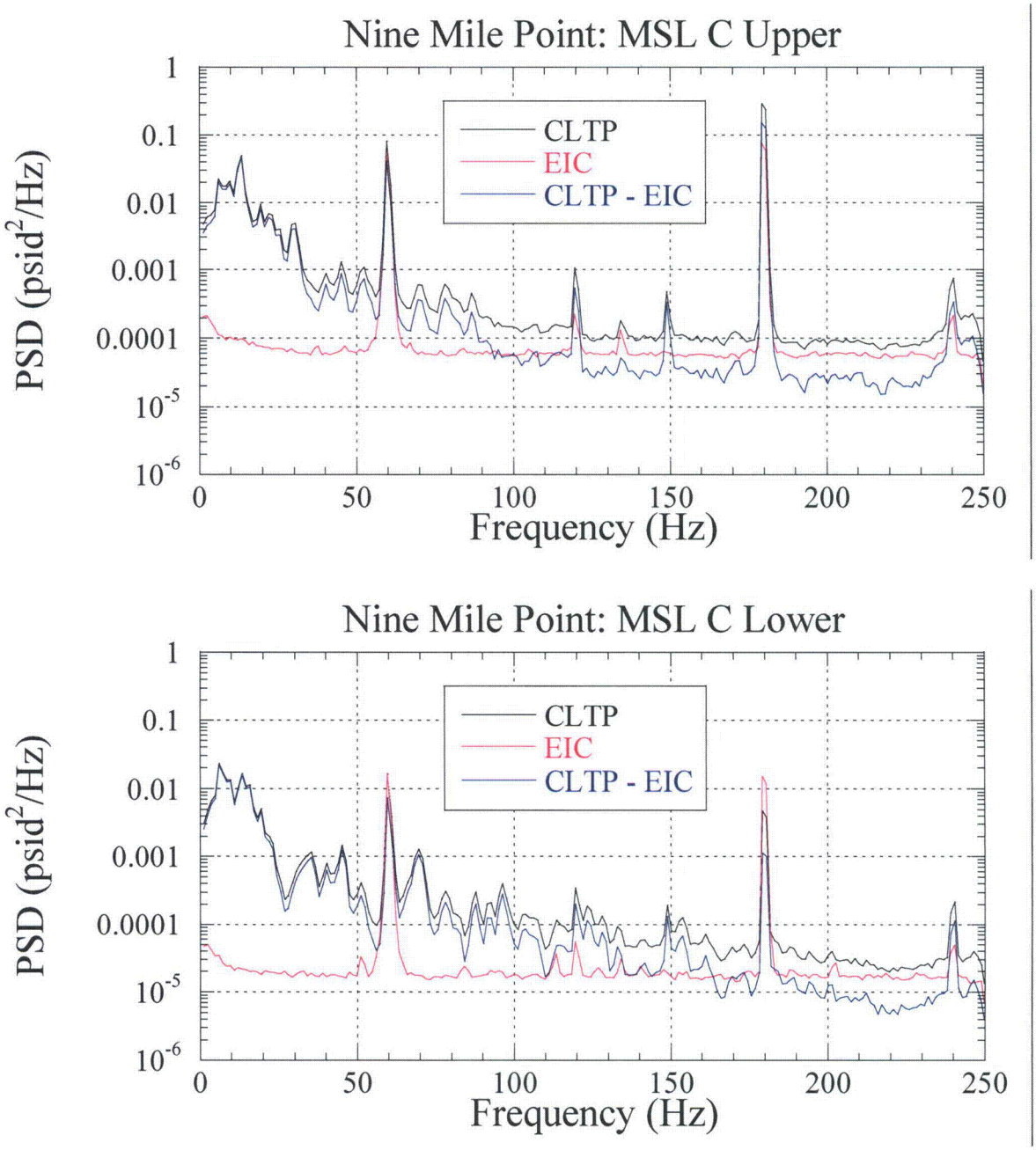

Figure 3.1c: Comparison of unfiltered data measured on the NMP2 main steam lines at CLTP conditions (black curves), EIC (red curves), and subtraction of EIC from CLTP (blue curves: MSL C Upper (top); MSL C Lower (bottom).

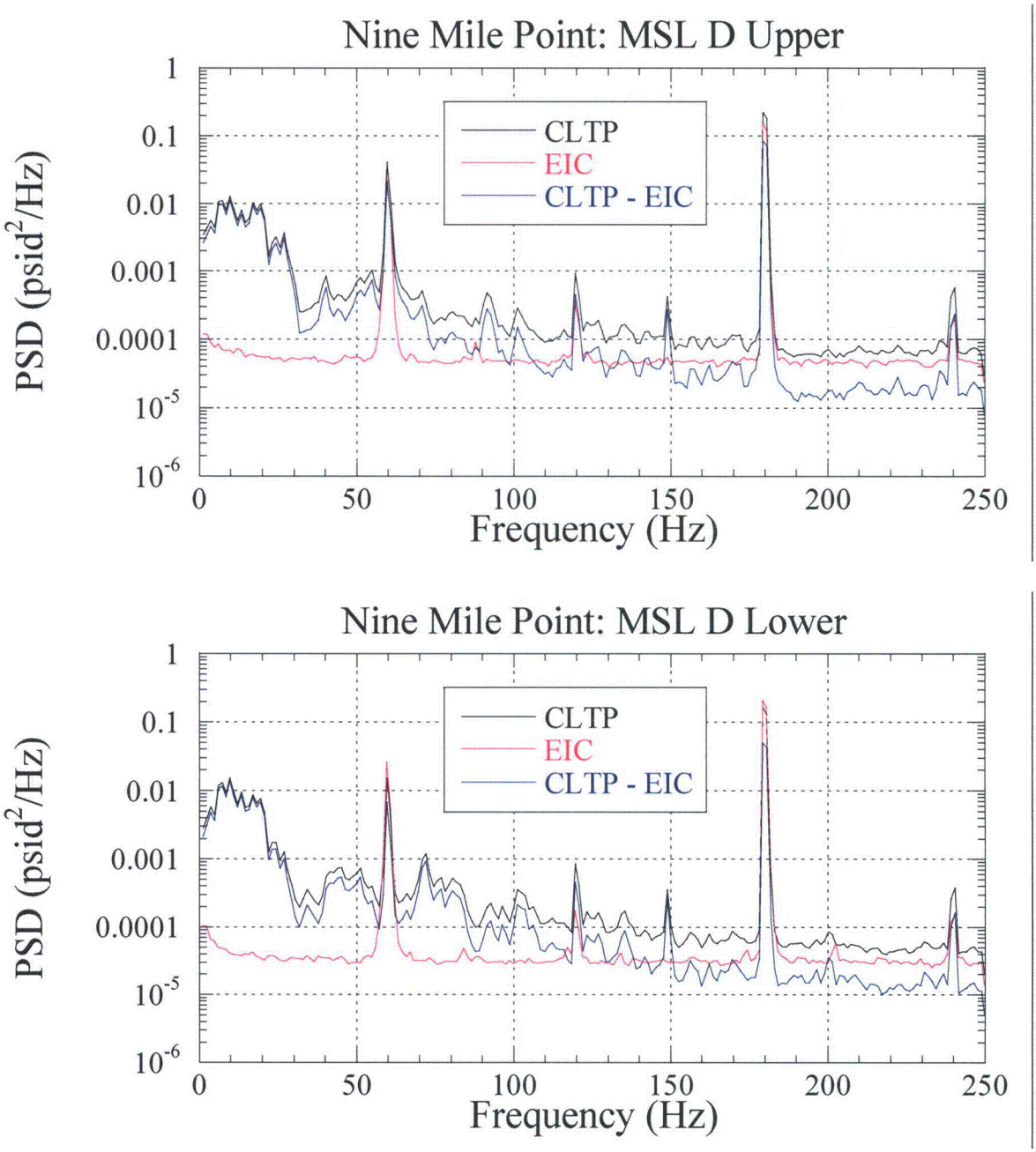

Figure 3.1d: Comparison of unfiltered data measured on the NMP2 main steam lines at CLTP conditions (black curves), EIC (red curves), and subtraction of EIC from CLTP (blue curves: MSL D Upper (top); MSL D Lower (bottom).

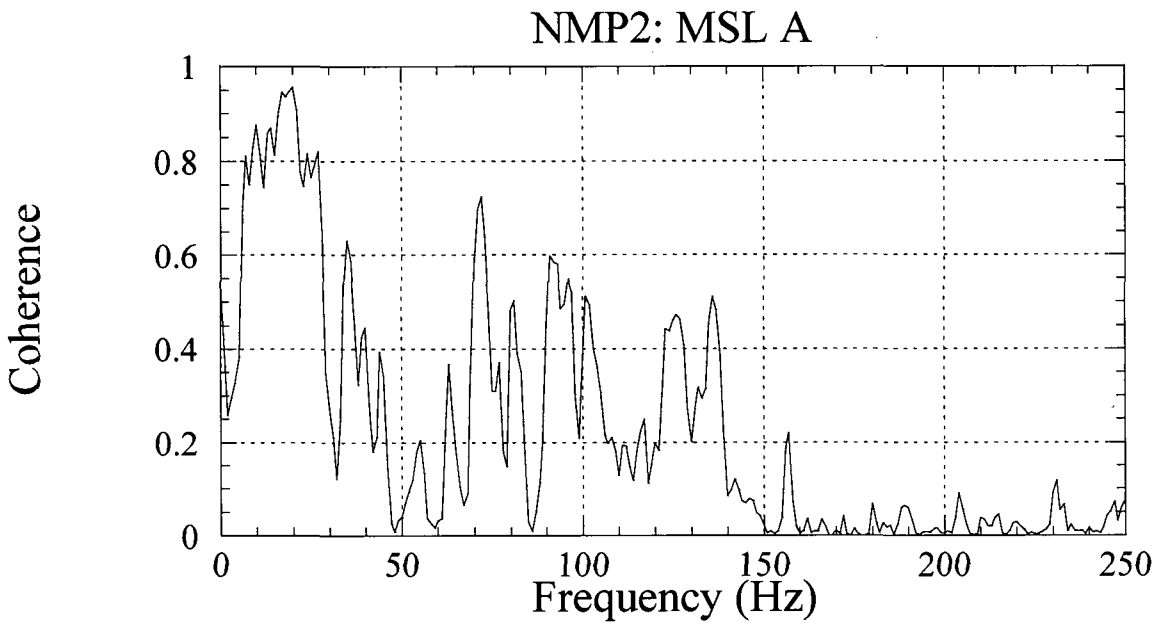

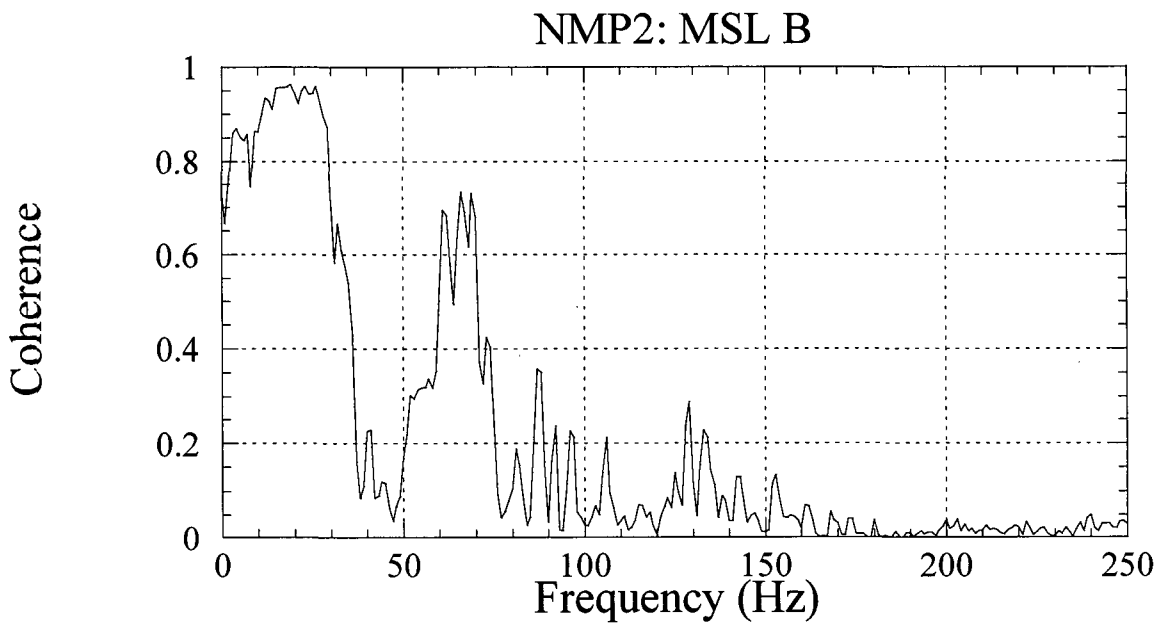

Figure 3.2a. Coherence between the upper and lower strain gage readings at NMP2: main steam line A (top); main steam line B (bottom).

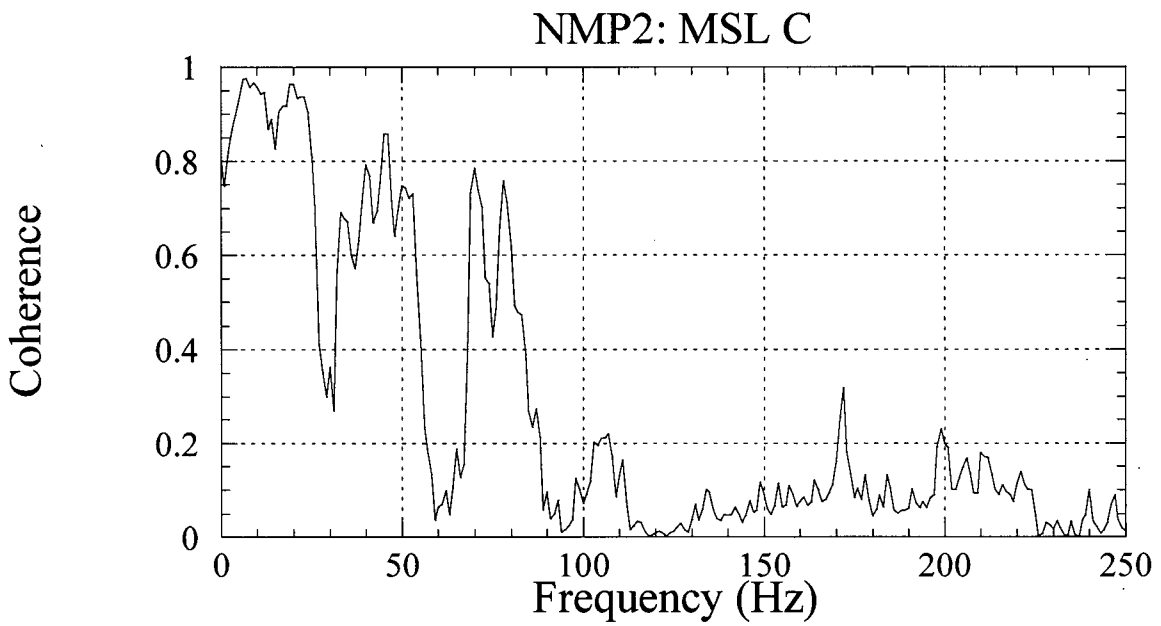

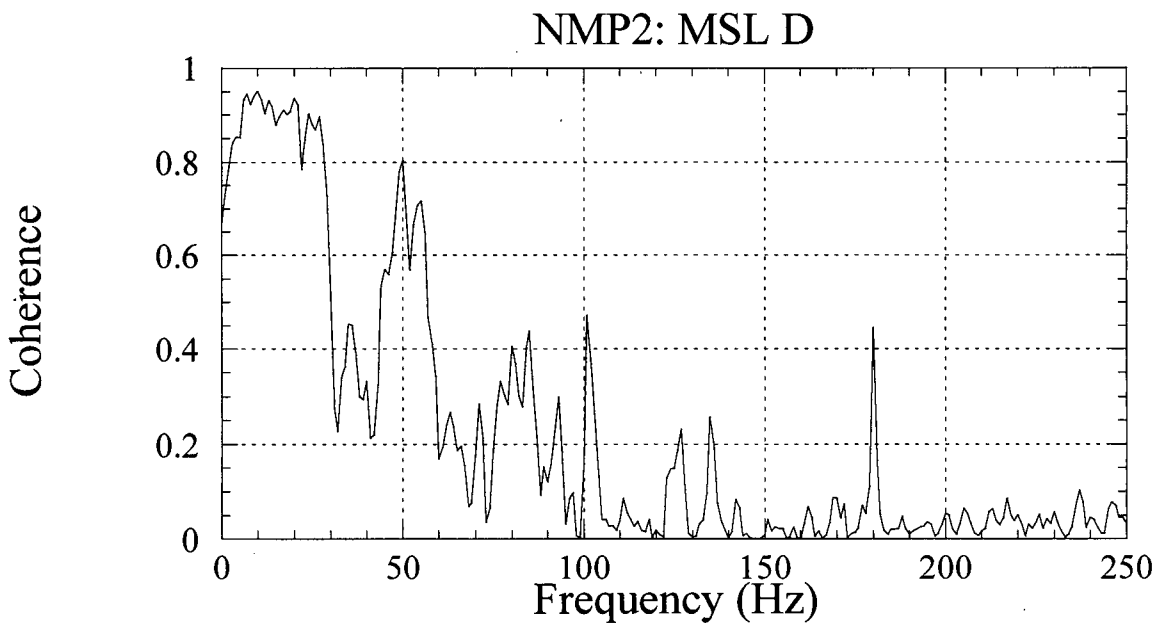

Figure 3.2b. Coherence between the upper and lower strain gage readings at NMP2: main steam line C (top); main steam line D (bottom).

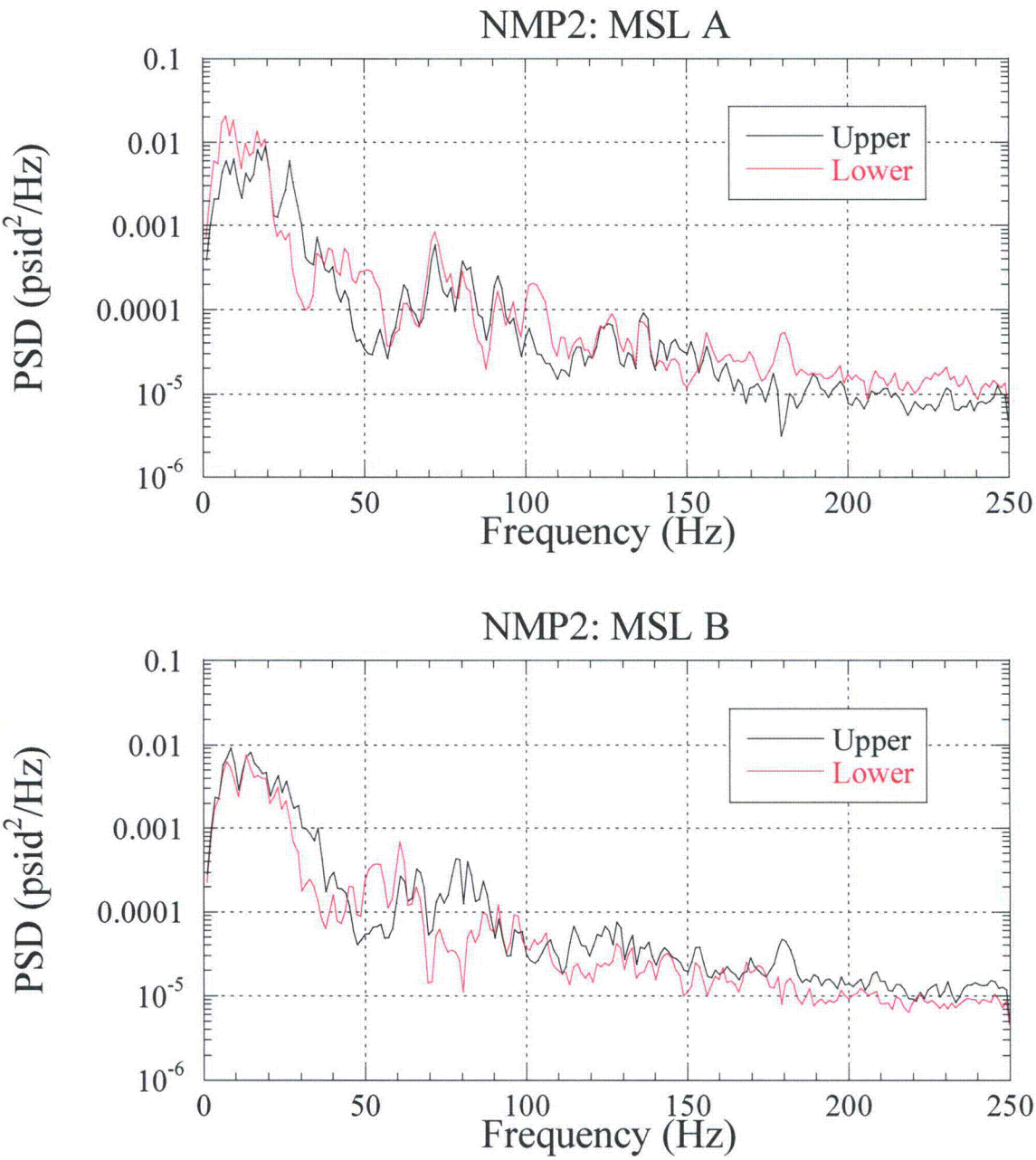

Figure 3.3a. PSD comparison of pressure measurements at strain gage locations on main steam line A (top) and B (bottom).

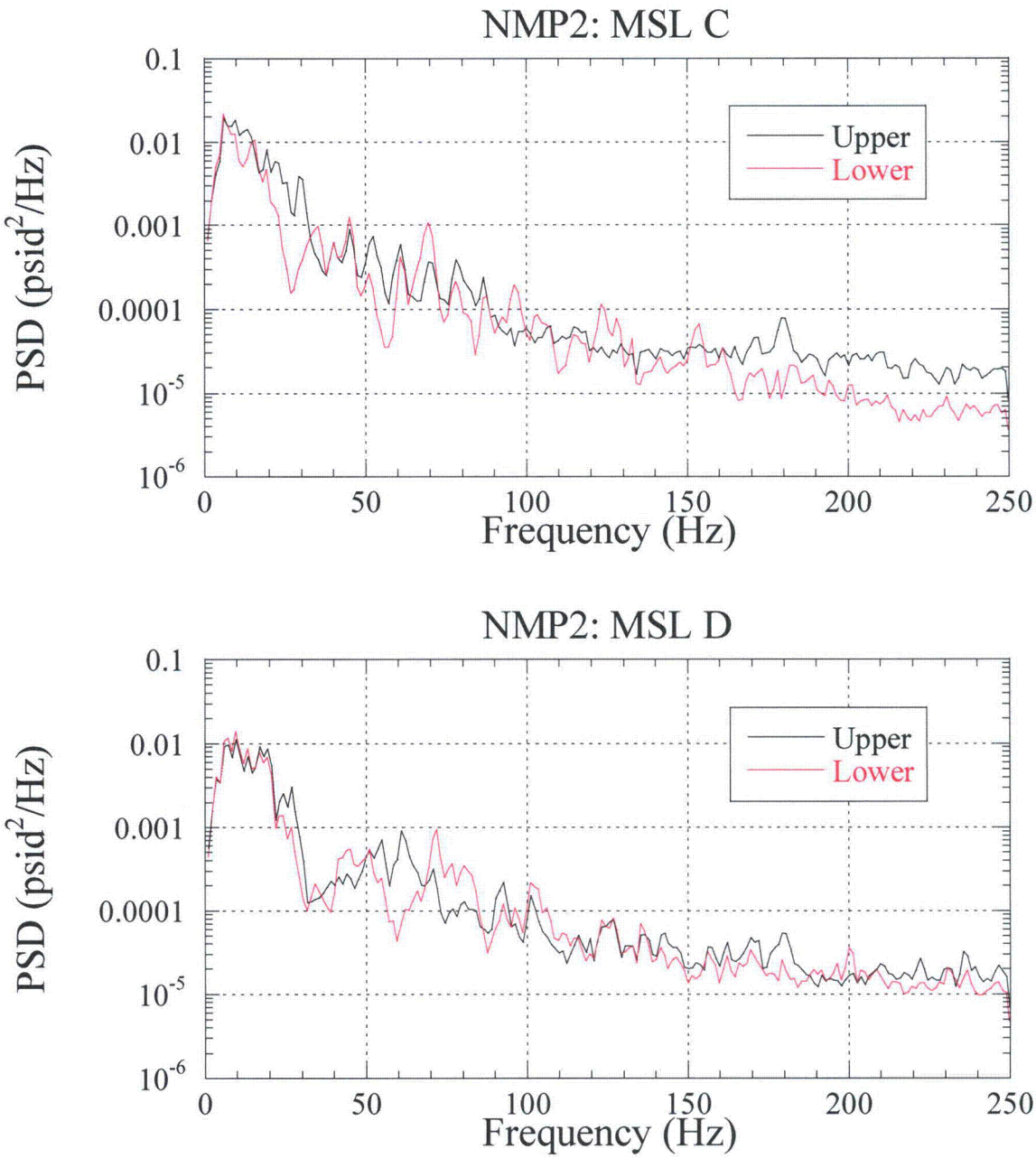

Figure 3.3b. PSD comparison of pressure measurements at strain gage locations on main steam line C (top) and D (bottom).

4. Results

The measured main steam line pressure data were used to drive the validated acoustic circuit methodology for the NMP2 steam dome coupled to the main steam lines to make a pressure load prediction on the NMP2 dryer. A low resolution load, developed at the nodal locations identified in Figures 4.1 to 4.4, produces the maximum differential pressure RMS pressure levels across the dryer as shown in Figure 4.5. PSDs of the peak loads on either side of the dryer are shown in Figure 4.6, while PSDs of the closure plate loads are shown in Figure 4.7.

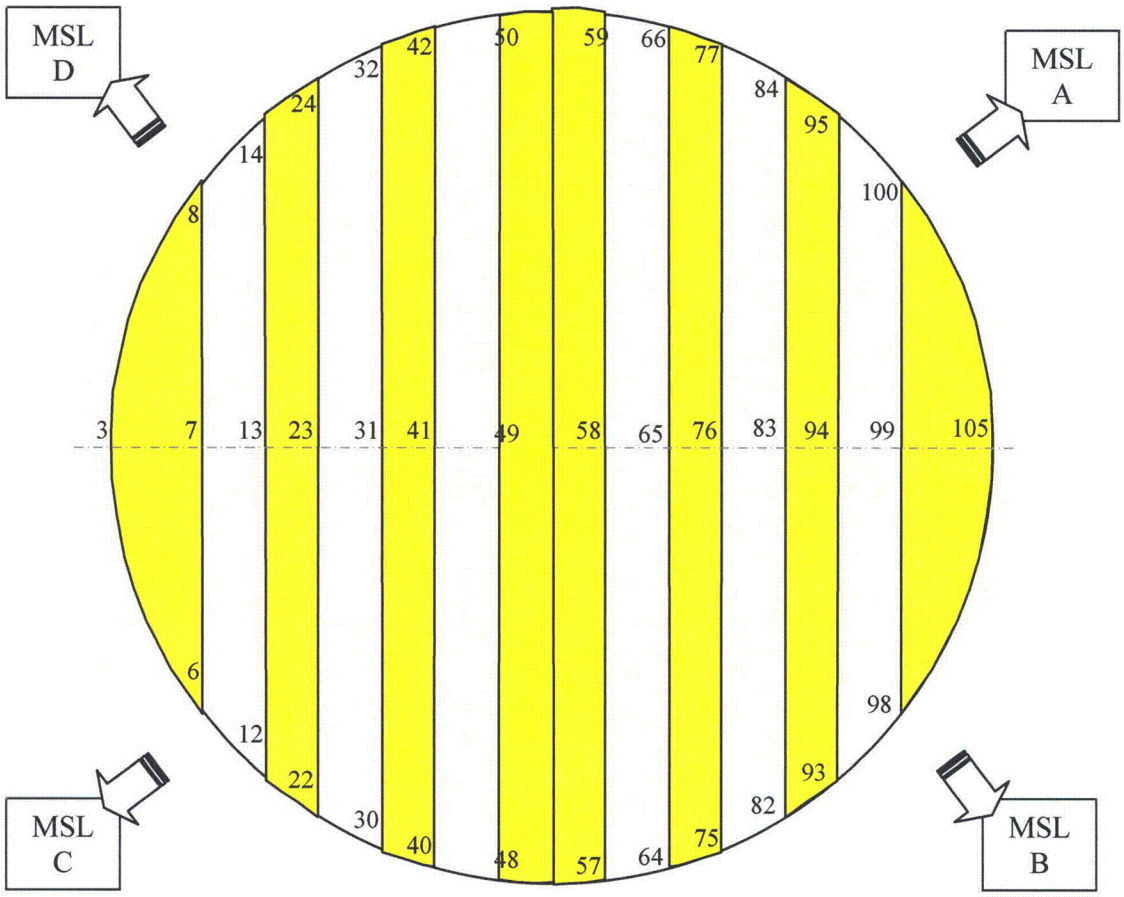

Figure 4.1. Cover and base plate low resolution load pressure node locations on the NMP2 dryer, with pressures acting downward in the notation defined here. Main steam line A is off the upper right corner of the figure; main steam line B off the lower right corner of the figure; main steam line C off the lower left corner of the figure; and main steam line D off the upper left corner of the figure. The cover plate on the A/B side of the dryer is identified by the nodes 98-99-100-105; the cover plate on the C/D side of the dryer is identified by the nodes 3-8-7-6. Base plates are identified by the nodes 64-65-66-77-76-75 and 82-83-84-95-94-93 (A/B side), 48-49-50-59-58-57 (center), and 12-13-14-24-23-22 and 30-31-32-42-41-40 (C/D side). The high resolution grid mesh (for subsequent finite element analysis) is spaced 3 inches on the cover plates, 6 inches on the first base plates, and 12 inches on the rest of the base plates.

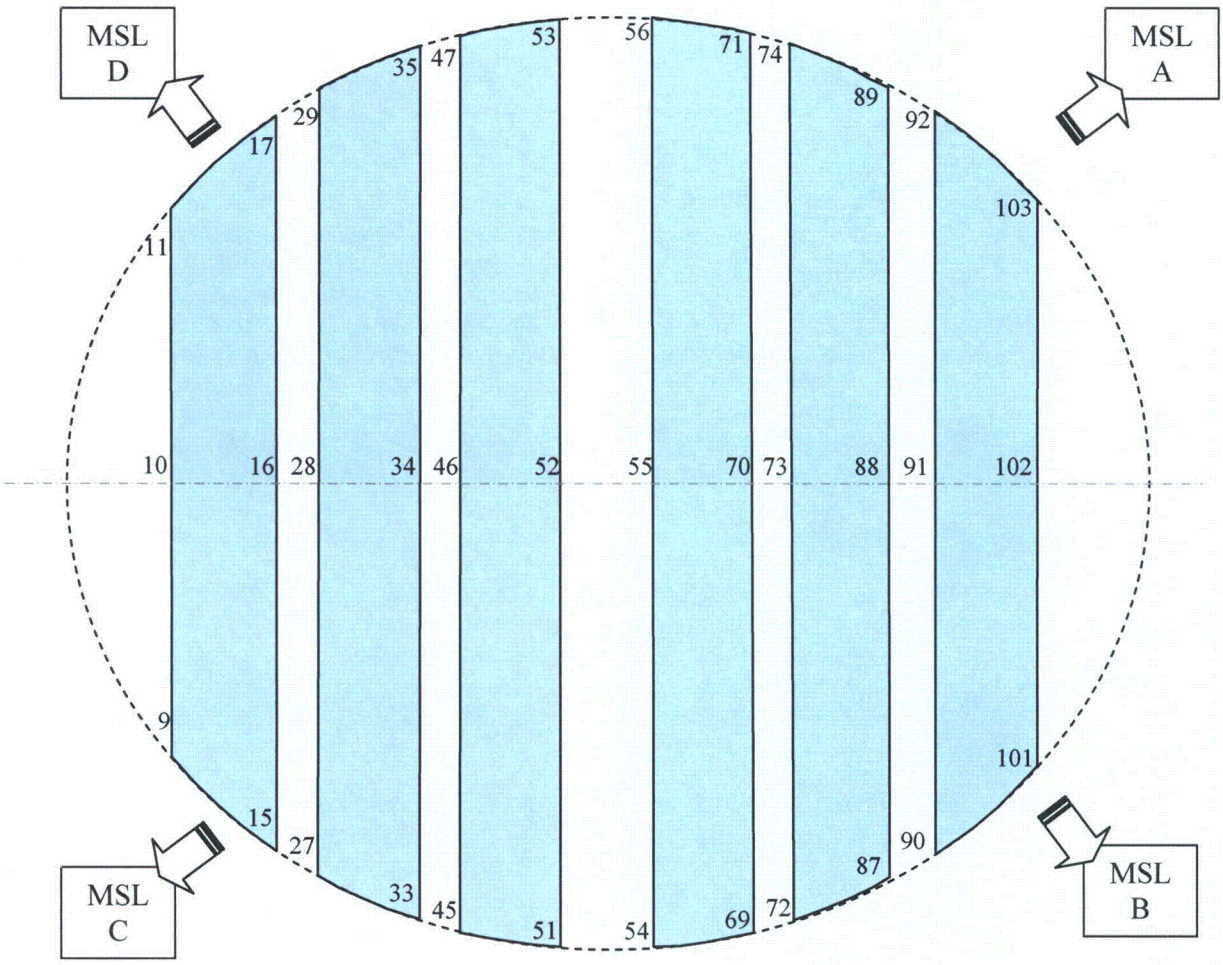

Figure 4.2. Top plate low resolution load pressure node locations on the NMP2 dryer, with pressures acting downward in the notation defined here. Main steam line A is off the upper right corner of the figure; main steam line B off the lower right corner of the figure; main steam line C off the lower left corner of the figure; and main steam line D off the upper left corner of the figure. Top plates on the A/B side of the dryer are identified by the nodes 90-91-92-103-102-101, 72-73-74-89-88-87, and 54-55-56-71-70-69. Top plates on the C/D side of the dryer are identified by the nodes 9-10-11-17-16-15, 27-28-29-35-34-33, and 45-46-47-53-52-51. The high resolution grid mesh (for subsequent finite element analysis) is spaced 3 inches on the outer top plates, 6 inches on the first inner top plates, and 12 inches on the rest of the inner top plates.

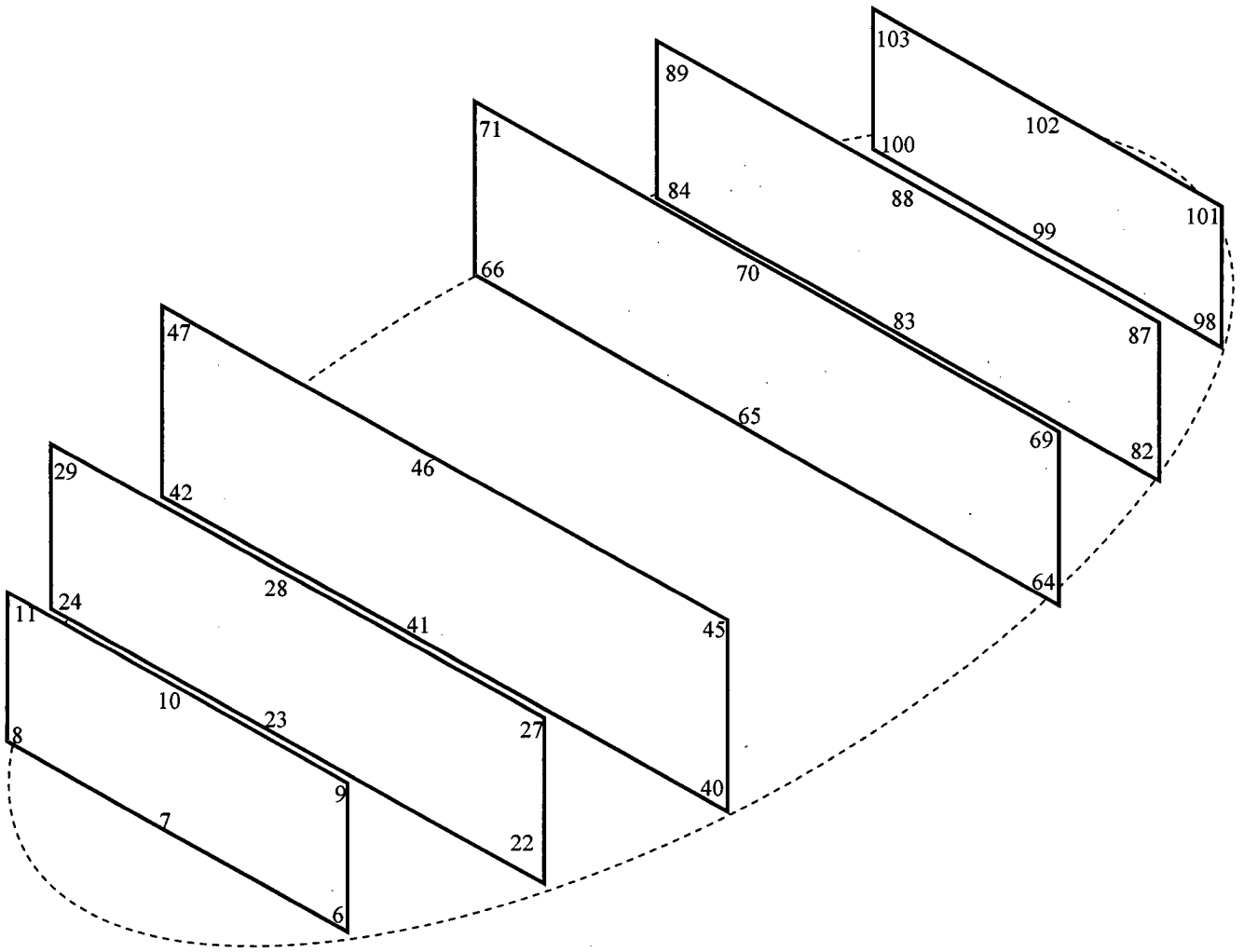

Figure 4.3. Outer and inner hood low resolution load pressure nodes on the NMP2 dryer. Main steam lines A and B are off the upper right corner of the figure; main steam lines C and D are off the lower left corner of the figure. Pressures act lower left to upper right on the outer hood identified by the nodes 6-7-8-11-10-9 (opposite C/D) and on the inner hoods identified by the nodes 22-23-24-29-28-27 and 40-41-42-47-46-45. Pressures act upper right to lower left on the outer hood identified by the nodes 98-99-100-103-102-101 (opposite A/B) and on the inner hoods identified by the nodes 82-83-84-89-88-87 and 64-65-66-71-70-69. The high resolution grid mesh (for subsequent finite element analysis) is spaced 3 inches on the outer hoods, 6 inches on the first inner hoods, and 12 inches on the inside hoods.

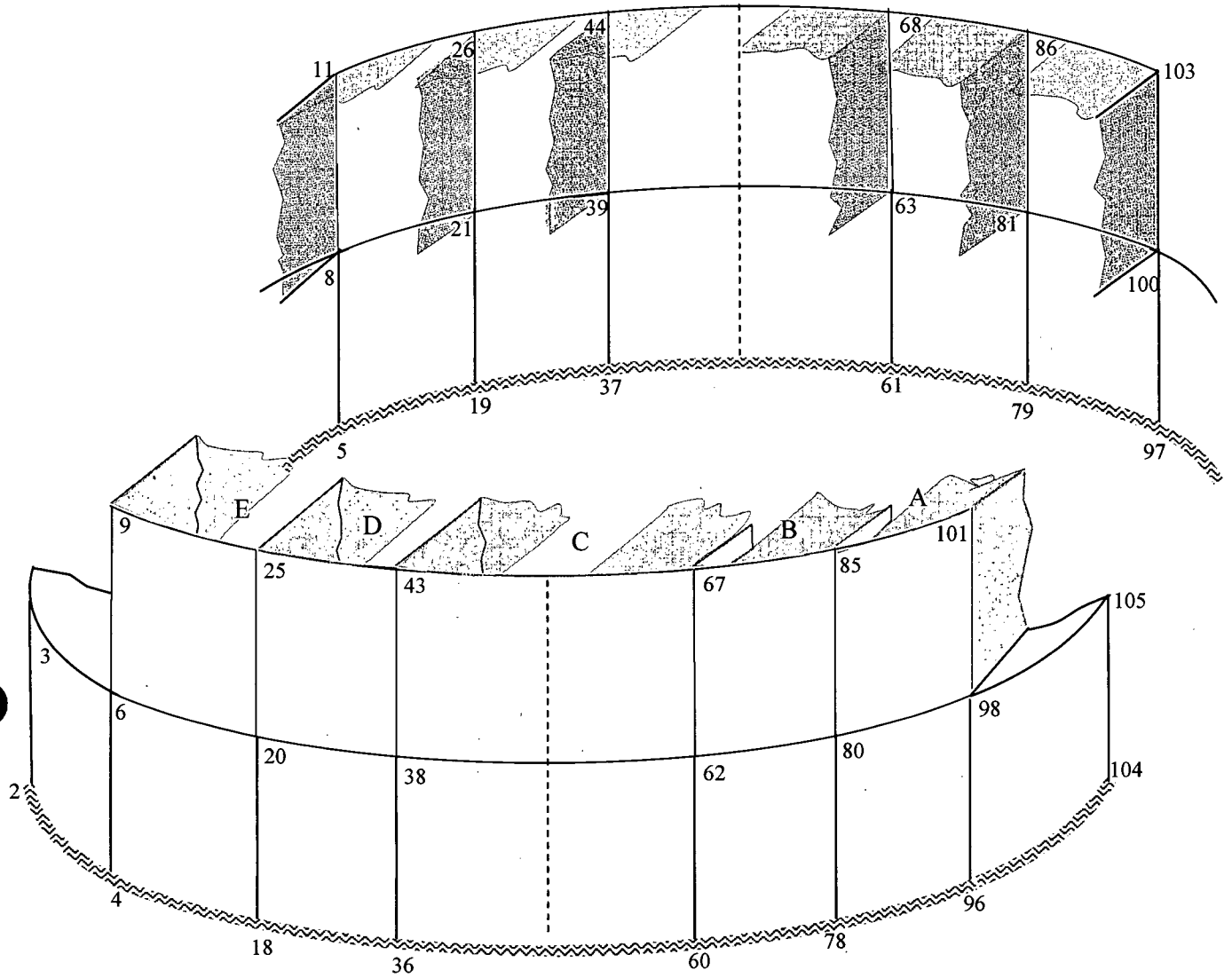

Figure 4.4. Skirt and end plate low resolution load pressure nodes on the NMP2 dryer, with pressures acting from the outside of the dryer to the inside. Main steam lines A and B are off the right side of the figure; main steam lines C and D are off the left side of the figure. Skirt nodes are 2-4-18-36-60-78-96-104 and 2-5-19-37-61-79-97-104. End plate nodes are 20-25 and 21-26, 38-43 and 39-44, 62-67 and 63-68, and 80-85 and 81-86. The high-resolution grid mesh (for subsequent finite element analysis) is spaced 3 inches on the outer portion of the skirt and end plates closest to the main steam lines, 6 inches on the sections nearer the center of the dryer, and 12 inches on the center of the dryer.

[[

(3)]]

Figure 4.5. Predicted loads on the low resolution grid identified in Figures 4.1 to 4.4, as developed by the Modified Bounding Pressure model, to 250 Hz. Low-numbered nodes are on the C-D side of the dryer, while high-numbered nodes are on the A-B side of the dryer.

[[

(3)]]

Figure 4.6. PSD of the maximum pressure loads predicted on the C/D side of the NMP2 dryer (top) and the A/B side (bottom).

[[

(3)]]

Figure 4.7. PSD of the closure plate pressure loads predicted on the C/D side of the NMP2 dryer (top) and the A/B side (bottom).

5. Uncertainty Analysis

The analysis of potential uncertainty occurring at NMP2 consists of several contributions, including the uncertainty from collecting data on the main steam lines at locations other than the locations on Quad Cities Unit 2 (QC2) and the uncertainty in the Modified Bounding Pressure model. QC2 dryer data at Original Licensed Thermal Power (OLTP) conditions were used to generate an uncertainty analysis of the Acoustic Circuit Methodology (ACM) [2] for NMP2.

The approach taken for bias and uncertainty is similar to that used by Vermont Yankee for power uprate [6]. In this analysis, six "averaged pressures" are examined on the instrumented replacement dryer at QC2: averaging pressure sensors P1, P2, and P3; P4, P5, and P6; P7, P8, and P9; P10, P11, and P12; P18 and P20; and P19 and P21. These pressure sensors were all on the outer bank hoods of the dryer, and the groups are comprised of sensors located vertically above or below each other.

Bias is computed by taking the difference between the measured and predicted RMS pressure values for the six "averaged pressures", and dividing the mean of this difference by the mean of the predicted RMS. RMS is computed by integrating the PSD across the frequency range of interest and taking the square root

$$\text{BIAS} = \frac{\frac{1}{N}\sum(\text{RMS}_{\text{measured}} - \text{RMS}_{\text{predicted}})}{\frac{1}{N}\sum \text{RMS}_{\text{predicted}}} \tag{5.1}$$

where $\text{RMS}_{\text{measured}}$ is the RMS of the measured data and $\text{RMS}_{\text{predicted}}$ is the RMS of the predicted data. Summations are over the number of "averaged pressures", or N = 6.

Uncertainty is defined as the fraction computed by the standard deviation

$$\text{UNCERTAINTY} = \frac{\sqrt{\frac{1}{N}\sum(\text{RMS}_{\text{measured}} - \text{RMS}_{\text{predicted}})^2}}{\frac{1}{N}\sum \text{RMS}_{\text{predicted}}} \tag{5.2}$$

ACM bias and uncertainty results are compiled for specified frequency ranges of interest, as directed by [7] and summarized in Table 5.1. Other random uncertainties, specific to NMP2, are summarized in Table 5.2 and are typically combined with the ACM results by SRSS methods to determine an overall uncertainty for NMP2.

Table 5.1. NMP2 bias and uncertainty for specified frequency intervals. A negative bias indicates that the ACM overpredicts the QC2 data in that interval.

[[

(3)]]

Table 5.2. Bias and uncertainty contributions to total uncertainty for NMP2 plant data.

[[

(3)]]

6. Conclusions

The C.D.I. acoustic circuit analysis, using full-scale measured data for NMP2:

a) [[

[3]]]

b) Predicts that the loads on dryer components are largest for components nearest the main steam line inlets and decrease inward into the reactor vessel.

7. References

1. Continuum Dynamics, Inc. 2005. Methodology to Determine Unsteady Pressure Loading on Components in Reactor Steam Domes (Rev. 6). C.D.I. Report No. 04-09 (Proprietary).

2. Continuum Dynamics, Inc. 2007. Bounding Methodology to Predict Full Scale Steam Dryer Loads from In-Plant Measurements, with the Inclusion of a Low Frequency Hydrodynamic Contribution (Rev. 0). C.D.I. Report No. 07-09 (Proprietary).

3. Nine Mile Point Unit 2 Drawings. 2007. Information provided in files 761E445AF, 197R624, 761E448, 761E448B, 3516-227-3, 0016010001729, 117C4972, 795E257, 921D597, 158B8534, 117C4519, 105D4673, and 795E260.

4. Structural Integrity Associates, Inc. 2009. Nine Mile Point Unit 2 Main Steam Line Strain Gage Data Reduction (Rev. 0). SIA Calculation Package No. NMP-26Q-302.

5. J. Ferrante. 2009. Evaluation of NMP2 Strain Gage Data for Attenuation Purposes (Rev. 0). Report No. JAFESC-09-02. Retained in C.D.I. Design Record File No. DRF-C-279E for Constellation Energy.

6. Communication from Enrico Betti. 2006. Excerpts from Entergy Calculation VYC-3001 (Rev. 3), EPU Steam Dryer Acceptance Criteria, Attachment I: VYNPS Steam Dryer Load Uncertainty (Proprietary).

7. NRC Request for Additional Information on the Hope Creek Generating Station, Extended Power Uprate. 2007. TAC No. MD3002. RAI No. 14.67.

8. Continuum Dynamics, Inc. 2006. Letter Report Documenting Onset Speeds and Frequencies Anticipated for FIV in Nine Mile Point Nuclear Station Safety Valve Standpipes. Our Ref. F459/0021 dated 08/16/06.

9. Structural Integrity Associates, Inc. 2008. Nine Mile Point Unit 2 Strain Gage Uncertainty Evaluation and Pressure Conversion Factors (Rev. 1). SIA Calculation Package No. NMP-26Q-301.

10. Continuum Dynamics, Inc. 2005. Vermont Yankee Instrument Position Uncertainty. Letter Report dated 08/01/05.

11. Exelon Nuclear Generating LLC. 2005. An Assessment of the Effects of Uncertainty in the Application of Acoustic Circuit Model Predictions to the Calculation of Stresses in the Replacement Quad Cities Units 1 and 2 Steam Dryers (Revision 0). Document No. AM-21005-008.

12. Continuum Dynamics, Inc. 2007. Finite Element Modeling Bias and Uncertainty Estimates Derived from the Hope Creek Unit 2 Dryer Shaker Test (Rev. 0). C.D.I. Report No. 07-27 (Proprietary).

13. NRC Request for Additional Information on the Hope Creek Generating Station, Extended Power Uprate. 2007. RAI No. 14.79.

14. NRC Request for Additional Information on the Hope Creek Generating Station, Extended Power Uprate. 2007. RAI No. 14.110.